the membrane. Our method may allow formation of micropores, and this alone could account for deviation of $\bar{P}_{O_2}$ from reported values. However, systematic errors introduced by the apparatus and the syringing techniques used in sampling may also contribute. Also our permeabilities were determined from a gas mixture rather than a single-component gas permeating through the membrane. Very few studies have been done on the permeation of gas mixtures through glassy polymers. However, in some cases deviations have been observed in permeabilities of pure penetrants vs. those in a mixture.[7] For our purposes, the important point is that consistent values were obtained so that polystyrene and the cobalt-complex-containing membranes can be compared with blanks and the difference in O_2 enrichment attributed to metal-promoted enhanced O_2 permeability.

With use of the permeation data from polystyrene membranes containing various loadings of dispersed functionalized polystyrene beads ($\bar{P}_{O_2} = (5.0 \pm 0.2) \times 10^{-10}$) a partial pressure vs. time curve is measured for an appropriate blank. We note here that a plot of partial pressure of oxygen vs. time for a cobalt (II)-containing membrane compared with the calculated curve for a blank in Figure 2 shows metal-promoted enhanced permeation of oxygen under approximately 16 mmHg of O_2. As the pressure of oxygen increases, we approach the $P_{1/2}$ for the complex and the cobalt is no longer effective for facilitating the transport of oxygen. The thermodynamics of oxygen binding to CoSMDPT in solution have been determined.[8] At 298 K $P_{1/2}$ is calculated to be 6.715×10^3 mmHg. Although comparison of binding constants of supported and solution complexes is not straightforward,[9] supported CoSMDPT in a polymer matrix appears to form a much more stable O_2 adduct than the solution analogue. ESR of the Co–O_2 adduct is still observed even after pumping on the film under a vacuum. When the cobalt is nearly completely oxygenated, O_2 is not removed from the low-pressure side of the film and the driving force for facilitated transfer of O_2 to that surface is removed. The O_2 adduct then functions to inhibit permeation through the film in comparison to the blank by removing free volume. This free volume is generally thought to be the diffusion pathway in the amorphous regions of the polymer. The intersection of the curves in Figure 2 reflects this loss of free volume. The usual mechanism[10] for facilitated transport involves diffusion of the carrier through the film. We have demonstrated facilitated transport in a system where the carrier does not have this mobility.

Substitution of the salicylidene portion of the SMDPT ligand with electron-withdrawing groups should decrease the electron density at the cobalt center as predicted by the spin-pairing model,[11] increasing $P_{1/2}$ for the complex. The oxygen permeation results for a polystyrene film containing polystyrene beads functionalized with the 3,5-Br_2SMDPT analogue are shown in Figure 3. Under approximately 24 mmHg of O_2 the cobalt is enhancing the permeation of oxygen. A slightly higher loading, 18% vs. 16% by weight, coupled with increased reversibility of the complex vastly improves the O_2 enrichment.

The polymer-bound CoSMDPT complexes can be cycled several times, and O_2 enrichment in the permeate gases is noted. However, ESR experiments indicate irreversible oxidation over several days. Studies are anticipated with site isolated silica bound CoSMDPT in order to improve recycling stability. In conclusion, we have demonstrated the enhanced O_2 permeation by polymer-bound CoSMDPT and are currently extending this work to other Co(II) and Fe(II) complexes as well as other polymer systems.

Acknowledgment. We thank the National Science Foundation (Grant No. 8408149) and the U.S. Army (Florida Technology Center) for their support of this research.

Registry No. Oxygen, 7782-44-7; polystyrene, 9003-53-6; (*N*,*N*-bis-(3-(salicylideneamino)propyl)methylamine)cobalt(II), 100313-46-0.

Department of Chemistry
University of Florida
Gainesville, Florida 32611

Russell S. Drago*
Kenneth J. Balkus, Jr.

Received October 11, 1985

---

[7] Chern, R. T. Ph.D. Thesis, North Carolina State University, 1983, and references therein.

[8] Drago, R. S.; Cannady, J. P.; Leslie, K. A. *J. Am. Chem. Soc.* **1980**, *102*, 6014.

[9] Drago, R. S.; Gaul, J. H. *Inorg. Chem.* **1979**, *18*, 2019.

[10] Way, J. D.; Noble, R. D.; Flynn, T. M.; Sloan, E. D. *J. Membr. Sci.* **1982**, *12*, 239.

[11] Drago, R. S.; Corden, B. B. *Acc. Chem. Res.* **1980**, *13*, 353.

Rhodium–Carbon Bond Formation by an Electrochemically Generated Monomeric Rhodium(II) Porphyrin Species

Sir:

The reaction of dimeric rhodium(II) porphyrins with alkyl halides and unsaturated olefins to form a rhodium–carbon bond was first characterized by Ogoshi.[1] These reactions have been postulated to proceed via the monomeric rhodium(II) radical [(P)$Rh^{II}\cdot$], where P is a porphyrin ligand.[2–4] In this case the initial reaction step is proposed to be homolytic dissociation of the Rh–Rh bond,[2,3] $[(P)Rh]_2 \rightleftarrows [(P)Rh\cdot]$. Monomeric Rh(II) porphyrin radicals have never been isolated, and most studies of rhodium(II) porphyrin reaction chemistry have utilized the dimeric complex. An electrochemically generated Rh(II) radical should show reactivity similar to that of the chemically generated Rh(II) if dimerization can be prevented. This is indeed the case, as presented in this communication.

Recently, we have shown that monomeric Rh(II) porphyrins can be quantitatively and quickly generated by electrochemical reduction of the Rh(III) porphyrin. The lifetime of these radicals depends upon both the temperature and nature of the axial ligands of the initial Rh(III) complex.[5] The electrochemical reduction of $(TPP)Rh(L)_2{}^+Cl^-$ where L = dimethylamine and TPP is the dianion of tetraphenylporphyrin is reversible at −78 °C and occurs as shown in eq 1. A reversible Rh(III)/Rh(II) reduction is not

$$[(TPP)Rh^{III}(L)_2]^+ \overset{e^-}{\rightleftarrows} (TPP)Rh^{II}(L)_2 \overset{e^-}{\rightleftarrows} [(TPP)Rh(L)_2]^- \tag{1}$$

observed for (TPP)Rh(L)Cl at this temperature nor is the first reduction of $(TPP)Rh(L)_2{}^+Cl^-$ reversible at room temperature, as shown in Figure 1a. This irreversibility is due to a chemical reaction following the generation of Rh(II), which in THF, benzonitrile, or pyridine forms $[(TPP)Rh]_2$.[5]

The reductive behavior of $(TPP)Rh(L)_2{}^+Cl^-$ in CH_2Cl_2 is different from that in benzonitrile, THF, or pyridine. A chemical reaction follows the first reduction, which, at a scan rate of 0.10 V/s, occurs at $E_p = -1.07$ V vs. SCE in CH_2Cl_2, but no dimer formation is observed in the cyclic voltammograms. Also, the product of the chemical reaction is reversibly reduced at −1.50 V, some 450 mV more positive than the reversible reduction potential of the dimer in benzonitrile. This is illustrated in Figure 1b.

Thin-layer spectroelectrochemistry was used to characterize the first and second reduction of $(TPP)Rh(L)_2{}^+Cl^-$ in CH_2Cl_2. After the first reduction, the Soret band shifted from 418 to 422 nm and the bands at 528 and 561 nm shifted to 535 and 566 nm. The electronic absorption spectrum of the first reduction product is consistent with formation of Rh(III).[6,7] After the second reduction, the bands at 422 and 535 nm decreased in intensity and a new band appeared at 604 nm, indicative of a porphyrin π-anion radical.

---

[1] Setsune, J.-I.; Yoshida, Z.; Ogoshi, H. *J. Chem. Soc., Perkin Trans. 1* **1982**, 983.

[2] Wayland, B. B.; Del Rossi, K. J. *J. Am. Chem. Soc.* **1985**, *107*, 7941.

[3] Paonessa, R. S.; Thomas, N. C.; Halpern, J. *J. Am. Chem. Soc.* **1985**, *107*, 4333.

[4] Wayland, B. B.; Woods, B. A. *J. Chem. Soc., Chem. Commun.* **1981**, 475.

[5] Kadish, K. M.; Yao, C.-L.; Anderson, J. E.; Cocolios, P. *Inorg. Chem.* **1985**, *24*, 4515.

[6] Wayland, B. B.; Newman, A. R. *Inorg. Chem.* **1981**, *20*, 3093.

[7] James, B. R.; Stynes, D. V. *J. Chem. Soc., Chem. Commun.* **1972**, 1261.

0020-1669/86/1325-0718$01.50/0

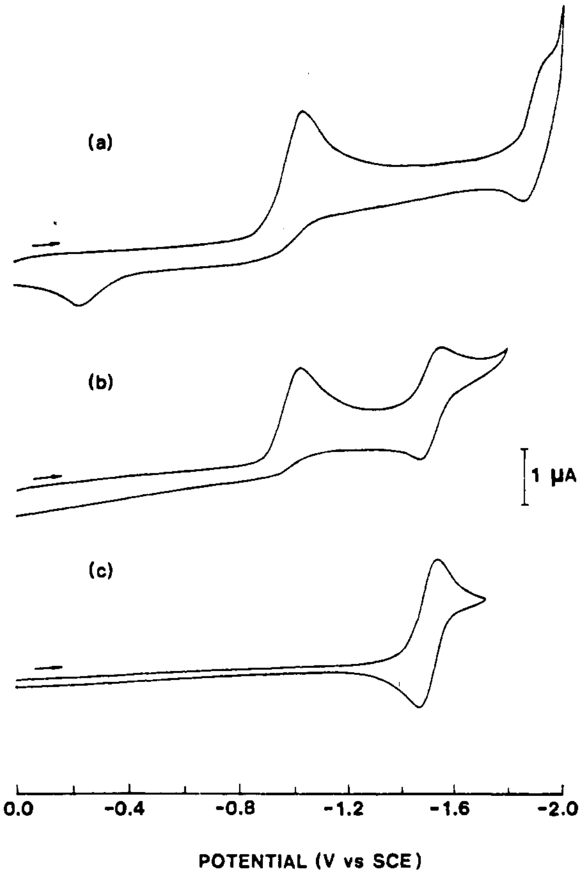

Figure 1. Cyclic voltammograms: (a) 9.9 × 10^{-4} M $(TPP)Rh(L)_2^+Cl^-$ in benzonitrile, 0.1 M TBAP; (b) 4.8 × 10^{-4} M $(TPP)Rh(L)_2^+Cl^-$ in CH_2Cl_2, 0.1 M TBAP; (c) 8 × 10^{-4} M $(TPP)Rh(CH_2Cl)$ in CH_2Cl_2, 0.1 M TBAP. All voltammograms were obtained at a scan rate of 0.10 V/s by using a Pt working electrode.

ESR measurements following bulk electrolysis of $(TPP)Rh(L)_2^+Cl^-$ agree with cyclic voltammetric and spectroelectrochemical measurements. After the first one-electron reduction, no ESR signal was observed. However, the second one-electron reduction of $(TPP)Rh(L)_2^+Cl^-$ resulted in a free-radical signal in the ESR; the *g* value was 2.00, and the signal width was 32 G.

The product of the chemical reaction following the one-electron reduction of $(TPP)Rh(L)_2^+Cl^-$ in CH_2Cl_2 was isolated and purified for characterization. All manipulations were performed under inert atmosphere by Schlenk techniques. A solution of $(TPP)Rh(L)_2^+Cl^-$ in CH_2Cl_2, 0.2 M TBAP, was bulk electrolyzed at −1.30 V for 30 min. The observed current decreased to background levels, indicating complete reduction. By current integration, 1.0 ± 0.1 e/Rh atom was required to complete the first reduction. The solution was removed from the electrochemical cell and vacuum-dried. The supporting electrolyte and any side products were separated from the product by using four acetonitrile extractions. The yield was nearly quantitative.

The main product from the chemical reaction following the first reduction of $(TPP)Rh(L)_2^+Cl^-$ in CH_2Cl_2 is $(TPP)Rh(CH_2Cl)$, which was characterized by infrared, UV–visible and ^1H NMR spectroscopy and by cyclic voltammetry. Cyclic voltammetric experiments (Figure 1c) confirmed that the isolated $(TPP)Rh(CH_2Cl)$ is the same species as that generated on the electrochemical time scale. The single reversible reduction of $(TPP)Rh(CH_2Cl)$ occurs at $E_{1/2} = -1.50$ V and is at a potential identical with that of the second reversible reduction of $(TPP)Rh(L)_2^+Cl^-$ in CH_2Cl_2. This potential is close to that of the first reduction of $(TPP)Rh(CH_3)$ in CH_2Cl_2.[8] The electronic absorption spectrum of the recovered product is identical with that recorded after the one-electron reduction of $(TPP)Rh(L)_2^+Cl^-$ in a thin-layer cell. The infrared spectrum of the recovered product does not indicate the presence of Rh–Cl or Rh–L (L = dimethylamine), nor does it indicate the presence of a $N(Bu)_4^+$ cation, a ClO_4^- anion, or the displaced dimethylamine.

The ^1H NMR spectrum of the recovered product in pyridine-d_5 demonstrates the formation of $(TPP)Rh(CH_2Cl)$. The porphyrin signals are at 8.99 (pyr H, singlet, 8 H), 8.29 (phenyl H, multiplet, 8 H), and 7.76 ppm (phenyl H, multiplet, 12 H), all relative to Me_4Si. A doublet (2 H) with peaks at −2.81 and −2.82 ppm is also observed and is assigned as the $Rh–CH_2Cl$ resonance. The J_{RH-H} coupling constant is 2.9 Hz. Proton resonances in this range are typical for Rh–CH signals. For example, $(OEP)RhCH(CH_3)OH$ has a Rh–CH signal at −2.4 ppm while $(OEP)RhCH(CH_2CH_3)OH$ has a signal at −2.34 ppm,[9] with splitting constants, J_{Rh-H}, of 3.5 and 3.25 Hz, respectively. $(OEP)Rh(CH_2C_6H_5)$ has a $Rh–CH_2$ signal at −4.57 ppm and a J_{Rh-H} splitting constant of 3.0 Hz.[1,10] Further examples of ^1H NMR characterization of rhodium porphyrin complexes containing a rhodium–carbon bond are in the literature.[1,11-13]

A small amount of $[(TPP)Rh]_2$ is observed in cyclic voltammograms of $(TPP)Rh(L)_2^+Cl^-$ in CH_2Cl_2, 0.1 M TBAP, taken at −25 to −50 °C or at very fast scan rates. However, dimer formation is not observed at room temperature (scan rates <1 V/s), nor is any dimer obtained from the bulk electrolysis, suggesting two competing process for $(TPP)Rh^{II}\cdot$. One process would be the reaction with another $(TPP)Rh^{II}\cdot$ molecule to generate a dimer; the second would be the reaction with CH_2Cl_2 to generate $(TPP)Rh(CH_2Cl)$. However, $[(TPP)Rh]_2$ also reacts with CH_2Cl_2 to form $(TPP)Rh(CH_2Cl)$, and hence, no dimer remains in solution.[14]

In summary, we have shown that electrochemistry is ideal for the generation of monomeric Rh(II) porphyrins and the monitoring of the reaction chemistry of this species. This electrogenerated radical may react with another Rh(II) radical to form a dimer or, in the presence of CH_2Cl_2, will react to generate the Rh^{III} complex containing a σ-bonded CH_2Cl group. Similar addition reactions with other alkyls and aryls are anticipated to occur. These reactions and mechanistic studies are now under investigation.

Acknowledgment. The support of the National Science Foundation (Grant No. 8215507) is gratefully acknowledged.

---

(8) $(TPP)Rh(CH_3)$ has one reversible reduction wave at −1.44 V and two reversible oxidation waves at 0.94 and 1.24 V vs. SCE in CH_2Cl_2, 0.1 M TBAP. $(TPP)Rh(CH_2Cl)$ has a single reduction at −1.50 V and two oxidation waves at 0.92 and 1.38 V vs. SCE.

(9) Woods, B. A. Ph.D. Dissertation, University of Pennsylvania, 1982.

(10) Pierce, R. M. Ph.D. Dissertation, University of Pennsylvania, 1983.

(11) Abeysekera, A. M.; Grigg, R.; Trocha-Grimshaw, J.; Viswanatha, V. *J. Chem. Soc., Perkin Trans. 1* **1977**, 1395.

(12) Ogoshi, H.; Setsune, J.-I.; Nanbo, Y.; Yoshida, Z.-I. *J. Organomet. Chem.* **1978**, *159*, 329.

(13) Ogoshi, H.; Setsune, J.-I.; Omura, T.; Yoshida, Z.-I. *J. Am. Chem. Soc.* **1975**, *97*, 6461.

(14) The chemical reaction between $[(TPP)Rh]_2$ and CH_2Cl_2 in benzonitrile or THF results in the quantitative formation of $(TPP)Rh(CH_2Cl)$. Since no (TPP)RhCl is formed, the reaction is probably between $(TPP)Rh\cdot$ and CH_2Cl_2 rather than direct reaction between CH_2Cl_2 and $[(TPP)Rh]_2$.

Department of Chemistry
The University of Houston—University Park
Houston, Texas 77004

J. E. Anderson
C.-L. Yao
K. M. Kadish*

Received September 20, 1985